Thermographic control of fingers and hands after replantation

by E. LAMBIRIS, A. SCHICK and H. STOBOY
Orthopedic University Hospital, Oskar-Helene-Heim. Berlin, (West Germany)

Summary. In 48 traumatic amputations of one or more fingers or of one hand, thermographic (T.) control investigation after replantation were carried out. T. is a reliable means of judging blood supply following replantation surgery.

Key words: thermography, replantations, blood flow.

AI INTRODUCTION

Recently, reports ‘were published concerning the replantation of traumatically amputated fingers or hands.[1,3] GAUDIN et al.[2] proposed to perform first the suture of arteries, and second the venous repair in order to shor‘ten the time of ischemia and to remove metabolic waste products. Thermographic (T.) controls of replantations have been carried out in addition to other diagnostic studies over a period of one yr.

The aim of this study is to document the course of surface radiation temperature to judge the blood flow in fingers and hands after replantation.

B) MATERIAL AND METHOD

The AGA 680 Medical Thermovision Device was used. The first T. investigation was performed immediately after the replantation. Room temperature was kept constant at 21°C. The patient rested 15 mins in the room prior to the investigation. The method detects changes of radiation temperature in the range of ± 1°C. Diminished blood supply causes decreased radiation temperature in the replantated finger. 48 replantations were performed; 29 after complete and 19 after incomplete amputations (Tab. I). Three cases of replantation relate to 2 instances of complete loss of the hand, and one of incomplete traumatic amputation of the hand. Control investigations were performed one wk, 2 wks, 3 months and 5 months after surgery.

Tab. I. **Distribution of complete and incomplete traumatic amputations of fingers and hands.**

Site	No cases	Traumatic amputation	
		Complete	Incomplete
Hands	3	2	1
Fingers	45	27	18
Total	48	29	19

C) RESULTS

The following results were obtained (Tab. II):

1. In the **first post-surgical investigation** done during the wk after operation, 15/48 patients presented hyperthermia due to hyperemia, 3/48 replants were normothermic. In 14/48 patients decreased heat radiation was noted. In 16/48 cases heat radiation was below normal ranges of isotherms.

2. After the **first and second wk,** results were virtually unchanged. One replant in which hypothermic measurements were in evidence, and 2 in which no temperature readings could be obtained had to be reamputated because of arterial or venous occlusion (Fig. 1). In one replant in which no T. readings had been obtained one wk after replantation, hypothermic readings were noted during the second.

Tab. 11. **Distribution of replants according to thermographic readings during the observation period. Out-of-range: no thermographic readings could be obtained due to a poor blood supply.**

Thermographic pattern	Periodical control					Surgical amputation
	After surgery	Wk		Month		
		1	2	3	5	
Hyperthermia	15	15	15	10	7	–
Normothermia	3	3	3	14	21	–
Hypothermia	14	14	14	8	4	2
Out of range	16	16	13	7	5	9
Total	48	48	45	39	37	11

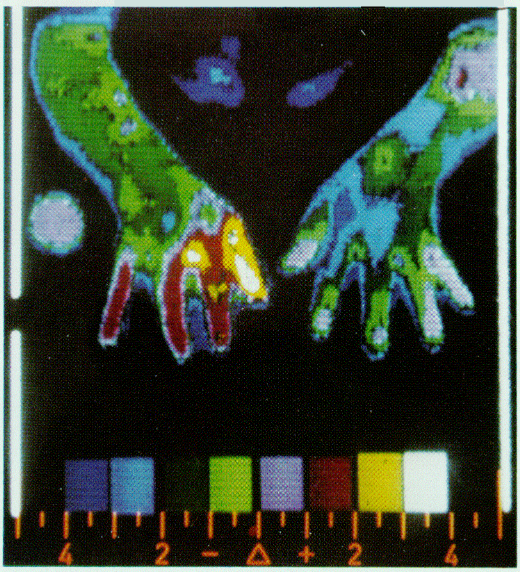

Fig. 1. After replantation no temperature readings of the 4th finger of the right hand could be obtained. In th 2nd wk a reamputation was necessary.

3. T. investigation in the **third month** after operation showed that 5 previously hypothermic (Fig. 2), 5 hyperthermic (Fig. 3) and one out-of-range cases were now normothermic. In one hypothermic and 5 out-of-range cases reamputation was necessary.

4. Five months after surgery an additional 7 replants were normothermic. Three of these had been previously hyperthermic, 4 hypothermic. Compared with the results obtained immediately after replantation, 21 cases presented normal temperatures. Two replants from which no T. readings could be obtained had to be reamputated. In 5 grossly hypothermic replants (Tab. II) amputation was not indicated not with standing poor blood supply. During the observation period under reference 11 amputations had to be performed.

D) DISCUSSION

According to the medical literature results of T. investigations of replantations have not been published so far. T. controls are important because differences of temperature may obtained from small areas of the replants. [redacted]esults of T. must be compared with clinical observations. Assuming that results obtained with T. indicate whether vascular anastomoses remain patent after replantation, a 66.7% success rate was achieved in the Authors' series (32/48). In the 10.4% in which out-of-range readings were noted, the outcome of the surgical procedure was uncertain. Some 22.9% (1 1/48) reamputations were necessary within the first 5 months. Complete occlusion of a vessel made visualization of the replantated finger in the T. picture impossible.

The ratio of success obtained by our surgical team was below that reported by MANDL et al" and BIEMER' (74.2% and 87%). These Investigators had examined a large sample of cases

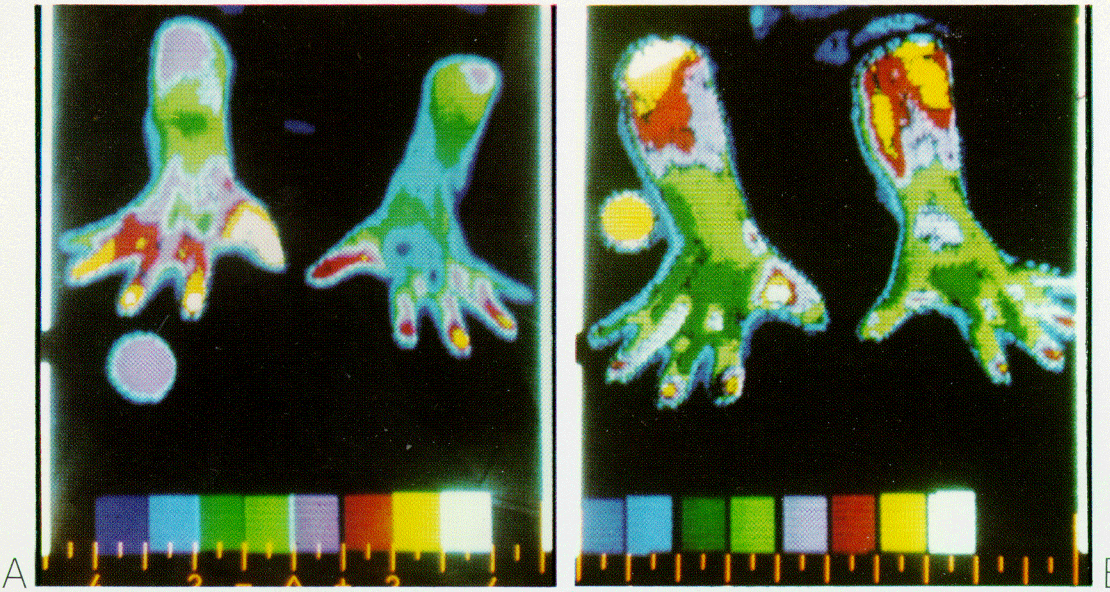

Fig. 2 A-B. A) T. after hand replantation. The left hand is distinctly hypothermic. B) Three months later the left hand is normothermic.

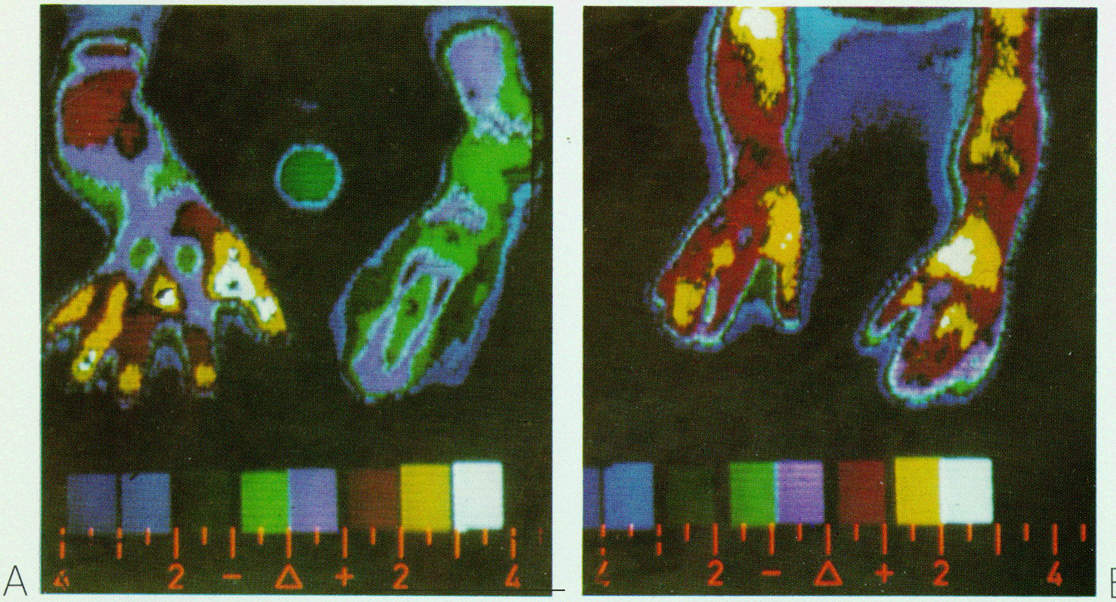

Fig. 3 A-B. A) T. after finger replantation. The right thumb is distinctly hyperthermic. B) Three months after surgery the right thumb is approximately normothermic.

but did not differentiate in the analysis of their results between finger, hand and arm replantation.

In the Authors' material none of the replants in the hyper- and normo-thermic range had to undergo reamputation. In 2 cases in which hypothermic readings were obtained after surgery, reamputation of the replant had to be carried out. In 9 cases in which reamputation proved necessary, no T. readings had been obtained.

REFERENCES

1. BIEMER E.: Replantation von Fingern und Extremitatenteilen. *Chirurg., 48, 353-359,* 1977.
2. GAUDIN B.P., ZILCH H., NEUBAUER M.: Replantation of the upper extremity. *Acta Orthop. Hellenica, 29,* 391, 1978.
3. MANDL H., FREILINCER G., HOUE H.: Replantationen im Handbereich mit ersten funktionellen Ergebnissen. Vortrag. Report at the *17th Congress of the Austrian Surgical Society,* Salzburg, 1976.

MTF measurement, a Simple method for determining the spatial resolution of a thermograph

by G.F. VERMEIJ,[1] M. ELAND[1] and J. STEKETEE[2]

[1] Department of Electrical Engineering, Twente University of Technology, Enschede. [2] Faculty of Medicine, Department of Biological and Medical Physics, Erasmus University, Rotterdam (The Netherlands)

Summary. By means of a thin heated wire and an oscilloscope with a delayed time base, the line-spread function (LSF) of a thermograph is determined. The sampled LSF points are Fourier transformed by a programmable pocket calculator, and the modulation transfer function (MTF) is calculated. The method has been tested on several infra-red cameras. Comparison of the results with earlier published measurements based on a rectangular modulation transfer method (bar chart) produces good reproduction with the LSF method and large numerical differences between the alternative ways of specifying the resolution of a thermograph. It is concluded that specification of the whole MTF should be adopted as a standardized way of specifying the spatial resolution of a (medical) thermograph.

Key words: spatial resolution, modulation transfer function, measurement, thermograph.

A) INTRODUCTION

As thermographs are being used more and more as measuring instruments in the medical field, the main specifications should be checked periodically. One of the parameters is the spatial resolution, represented by the system modulation transfer function (MTF). This is a generally accepted and physically sound way of expressing the spatial resolution of (IR) optical instruments.*

The MTF test method described in this paper was designed for simplicity and for use in a non-specialized technical environment. It only requires an oscilloscope with delayed time base, (possibly) a photo camera, a piece of thin electrical resistance wire (NiCr; ø < 0,3 mm) and a supply to deliver its heating current. A programmable pocket calculator such as Texas Instruments SR 56, TI 59, Hewlett Packard HP 65, 67,97, or a desk top calculator completes the list of requirements.

The measurement is performed on the videosignal and excludes the display transfer of the thermograph.

B) THE MODULATION TRANSFER FUNCTION (MTF)

To define the MTF of a thermograph, an object temperature pattern is chosen in which the radiation intensity varies sinusoidally, as measured along a certain line in the object. The intensity in the image also varies in the same manners. The absolute value of the ratio of the sine wave amplitudes of the image intensity and the original object are plotted as a function of the sine frequency and this is called the Modulation Transfer Function (MTF).

Frequency here refers to the number of sine periods per unit length. The laws of FOURIER transformation yield that every image can be described by a certain set of sinusoidal modulated functions. In general, large sized objects are represented by a set of mainly low-frequency functions (in the frequency domain) while the small sizes correspond to higher frequencies. In Fig. 1, 2 typical normalized MTFs are given.

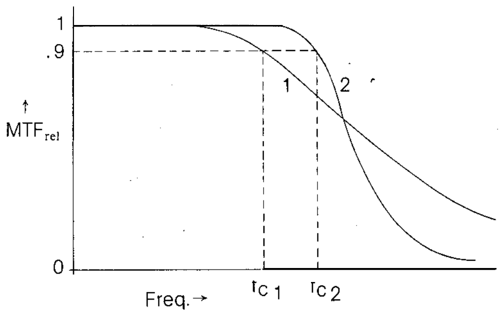

Fig. 1. Two typical relative MTF curves.

It must be emphasized that a thermograph is commonly calibrated with large sized references. This means that the scaling factor is adjusted for the low frequency (flat) part of the MTF. Hence, an MTF attenuation of 10% at frequency f_c gives rise to a measuring error of -10%. For general medical application this error seems to be acceptable. However, much of the object detail, corresponding to frequencies beyond f_c, is easily perceptible and presumably important for detection purposes. However, these frequencies cannot be measured quantitatively without great error. Due to these phenomena, a very sharp detented thermogram caused by the long tailed MTF 1 of Fig. 1 is inferior for quantitative purposes to the thermogram that lacks the photographic sharpness of 1 but has been recorded by an instrument with MTF 2 of Fig. 1.

The mathematical expression for the MTF is given by:

$$\mathrm{MTF} = \left| \int_{\infty}^{\infty} L(x) \exp(-2\pi i x f_x)\, dx \right| \qquad (1)$$

with L(x) the system response on a one-dimensional line-shaped object (line spead function)
the distance usually in the image plane
f_x the frequency in cycles/unit distance
i the imaginary unit /i = -1

Usually, the relative MTF is specified for an instrument as:

$$\mathrm{MTF}_{rel} = \frac{\mathrm{MTF}}{\int L(x)\, dx} 100\% \qquad (2)$$

with the property that for $f_x = 0$, $\mathrm{MTF}_{rel} = 100\%$.

The system MTF can be determined directly based on frequency by measuring the response on sinusoidal test patterns at different spatial frequencies. Because construction of a sinusoidal test pattern is complicated, one often resorts to a pattern of rectangular bar.[4] In this case, a transfer function is determined which is approximately equal to the MTF but gives significant differences for lower frequencies, as will be shown later. According to formula (l), a second method for measuring the MTF can be made by using a heated wire as a test pattern. When the line-spread L(x) is measured, the normal MTF can be calculated in which both formulae (1) and (2) are taken into accent.

The application of Discrete FOURIER Transformation to (2) yields:

$$\left| \frac{\sum^{m} L(x_j) \cdot \cos 2\pi f_x x_j}{\sum_{j=1}^{m} L(x_j)} \qquad \frac{\sum^{m} L(x_j) \cos 2\pi f_x x_j}{\sum_{j=1}^{m} L(x_j)} \right|$$

with $L(x_j)$ the LSF samples equally spaced on the x-axis at a distance Ax, see Fig. 2.

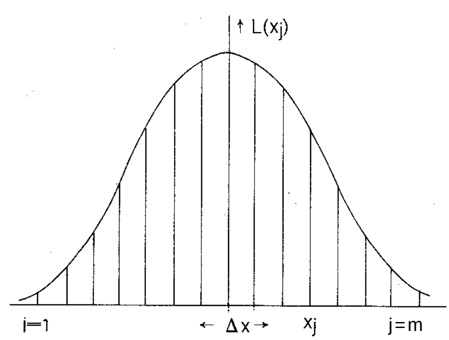

Fig. 2. Equally spaced sampling of LSF.

Recently, a simple and straight-forward programme based on the HP 65 calculator has been published.[3]

This programme can be used to obtain the MTF in a few mins. The same algorithm is programmed for other calculators and a programme used on a Texas Instruments TI 59 is available on request. When $2\pi f_x x_i$, x_i is chosen to represent distance increase Ax in mm in the image, the MTF frequency f_x is expressed in line pairs or cycles/mm. When the angular increment is chosen in radians, cycles/radians are expressed in the result.

CI EXPERIMENTAL SET-UP

Fig. 3 gives a schematic impression of the experimental set-up. A blackened electrical resistance wire is heated by the current of a power supply. This represents the line source. A second line source is fastened at a fixed and known distance d to provide the right scaling factor. The camera is focused and positioned so that the scanning lines are perpendicular to the image of the line source. The distance 1 from the wire to the lens centre is measured.

An oscilloscope with a delayed time base generator is used. The time base starts after an adjustable delay of the V-pulse (frame). This delay is chosen such that the 2 line sources are both visible in the video signal (for a slow time base). This yields the number of cm per micro-second. When the time base is set faster until the LSF of one of the line sources appears, a photograph is taken from the screen and the time base scale is noted. The LSF scaling factor is then easily determined. Examples of an LSF photo are given in Figs. 4A and 4B. This photo of L(x) is then sampled by hand by dividing the time (distance) axis into equal parts. The parts are chosen so as to result in a total number of 9-17 points. This will deliver sufficient accuracy.'

D) RESULTS

The described set-up and procedure were used to measure the MTF of several thermographs: Bofors Mark III, AGA 680 with 10" lens, AGA 750 with 7" and 20" lenses. The measured MTFs are shown in Fig. 5.

E) DISCUSSION

The camera types and object distances chosen were the same as those used by STEKETEE.[4] Comparison of his M-functions with the MTFs measured by the Authors is in principle impossible because they characterize different things. However, there appears to be a striking

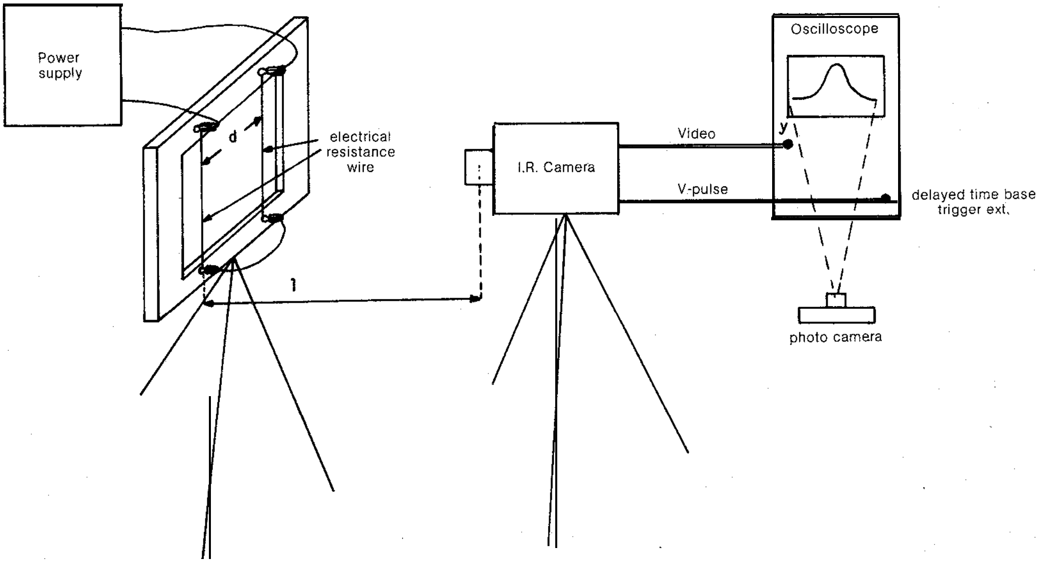

Fig. 3. Experimental set-up.

A

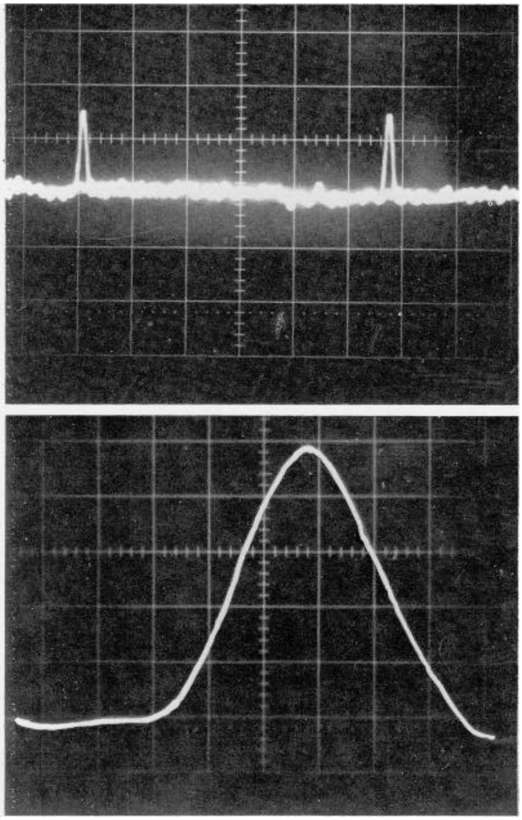

B

Fig. 4 A-B. A) Bofors Mark 111, object distance 1.60 m., time base 20μ s./div. d = 9 cm. B) Bofors Mark III, object distance 1.60 m., time base 1μ s./div.

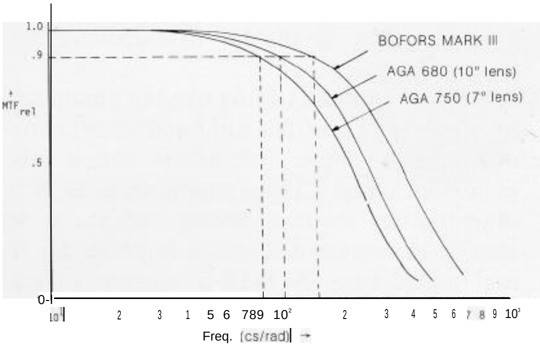

Fig. 5. Relative MTFs, object distance 1.60 m.

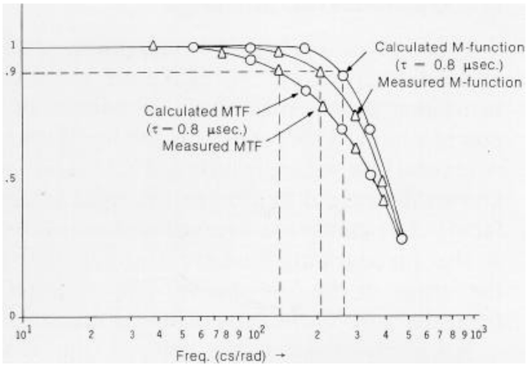

Fig. 6. Calculated (0) and measured (A) normalized M-function and MTF for a Bofors Mark III camera, object distance 1.60 m.

numerical difference between both transfer function types for a considerable part of the frequency domain. To answer the question whether this MTF measurement is traceable to the M-function or not, both transfers have been calculated for the same camera: the Bofors Mark III. This choice was made because the same apparatus was available as that used by STEKETEE in 1974.[4] The camera transfer was modelled by a convolution of a rectangular modulation function M, of 6 periods of varying frequency, with a rectangular detector window function W and an exponential impulse response $e^{\frac{-t}{\tau}}$, representing a first order low pass behaviour of the video preamplifier. The top value transfer for different frequencies of M delivers the M-function. The same is done with a sinusoidal modulation (instead of&I). The result is the MTF. The results of this approach are indicated in Fig. 6 by (0).

The agreement between the calculated and the measured characteristics for this camera appears to be very good. This proves that the described simple MTF measurement method is fully traceable to the earlier M-function method on the condition of validity of the model.

F) CONCLUSIONS AND RECOMMENDATIONS

1. There appears to be a **large numerical difference between** the M-function and the MTF. Especially at the 90% transfer point, the corresponding frequency in the rectangular case can be almost twice that of the sinusoidal one.

2. The described MTF measurement **method is fully traceable to rectangular** modulation measurements published earlier and is

easy to carry out with standard technical service instrumentation.

In optics the MTF curve is generally understood to be an unambiguous and versatile way of specifying spatial resolution. This is due to the fact that in the frequency domain the MTFs of parts of a system parts can be multiplied for every frequency point to obtain the total system MTF. Because this is not applicable to the M-function, the spatial resolving power of a thermograph should be specified by giving the total MTF curve. When this is done in a standardized way, the user may compare the performances of different cameras in a more meaningful way.

REFERENCES

1. ELAND M.: *Een eenvoudige MTF-meetmethode voor infrarood thermografen*. B. report TM 79-017. Group M & I, Dept. El. Engineering, Twente University of Technology, Enschede, the Netherlands.
2. LLOYD J.M.: *Thermal Imaging Systems*. Plenum Press, New York and London, 1975.
3. RONAI P.M., KIRCH D.L.: Rapid, rigorous computation of modulation transfer function on a pocket calculator. *J.N.M.*, **18**, 579-583, 1977.
4. STEKETEE J.: *Spatial resolution of thermographic cameras*. Thermography, Proc. 1st Europ. Congr., Amsterdam, 1974.

Calculation of the effects of oedema on breast thermograms

by U.R. BARKER

School of Mathematics, University of Bath, Bath (U.K.)

Summary. Calculation shows that oedema between a tumour and the skin surface will generally reduce the rise in temperature at the skin, but it may still be possible to detect the tumour by the abnormal vascularity produced.

Key words: thermography, tumours, oedema.

A) INTRODUCTION

A theoretical study of heat flow in breasts, with reference to the detection of tumours by thermography (T.) was made in 1976.' It has been pointed out that tumours are often associated with oedematous tissues, so this paper extends the calculations to such a case. The description of oedema, which has to be incorporated in the mathematical model, was obtained in discussions at the Anglo-Dutch Thermographic Society's meeting at Gateshead, U.K., on the 6th cf October 1979.

ACKNOWLEDGMENT. *The problem was suggested by Dr.* AGNES M. STARK, *Queen Elizabeth Hospital, Gateshead, U.K.*

B) MODEL OF BREAST WITH TUMOUR

The geometric form of the model is a very simple one (Fig. l), in which the boundaries between regions are parallel planes. First, there are 2 mm of dermis, then 2 mm of fatty tissue behind which lies the tumour in an anarchic hyper-vascularised region which is taken as being at 37°C. The skin is exposed to the air, as in a breast clinic, and it is given enough time to reach thermal equilibrium with an ambient temperature of 20°C. The resulting skin temperature is calculated using the tissue data given in Tab. I. For Fig. 1A it is 34.5°C compared with 29.3°C for a «normal» breast modelled in Fig. 1E.

Some or all of the 2 mm of fatty tissue is now made odematous as in Fig. 1 B-C-D. This

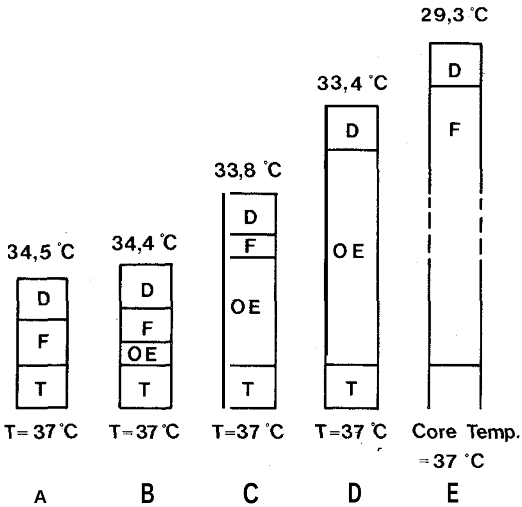

Fig. 1 A-B-C-D-E. Equilibrium skin temperatures when exposed to 20°C ambient. A) Tumour (T) at 37°C, behind 2 mm fatty tissue (F) and 2 mm dermis (D). B) The fatty tissue is gradually exchanged for oedematous tissue (OE); 1,8 mm fatty tissue and 1 mm of oedema. C) The fatty tissue is 1 mm thick, while the oedematous tissue is 5 mm thick. D) No fat, only 10 mm of oedema. E) «Normal» breast: 2 mm dermis and 38 mm fatty tissue. The skin temperature, in equilibrium with an ambient temperature of 20°, is 29,3°C.

change involves distension of the fatty tissue, represented by increasing the thickness 5 times, and decreasing the perfusion and metabolic heating rates for fat (Tab. I) by dividing them by 5. All these changes act to reduce the skin temperature. Finally, the thermal conductivity is increased to the value for water. This last change will tend to increase the skin temperature but, as the results show, the overall effect of the 4 changes is a drop in skin temperature.

In fact, the role of perfusion and normal metabolic heating of the tissue is negligible throughout Fig. 1 because the region at 37°C is so near to the skin; on the other hand, omitting both from Fig. 1E where the hot core is 40 mm deep would reduce the skin temperature by 3.8 "C. In conditions where blood perfusion and metabolic heating can be neglected, oedematous tissue will tend to hide the tumour if its thermal resistance is greater than that of the fatty tissue from which it is derived. This will be so if the expansion in thickness is greater than k_O/k_F times, where these are the thermal conductivities of the two kinds of tissue. In the present case, this would be an expansion in thickness by 0.62/0.25 = 2.5 times.

C) DISCUSSION

The detection of the tumour by its direct effect in elevating the skin temperature becomes rapidly less likely as its depth is increased,' and oedema will also help to hide it. A spherical tumour, rather than an extensive flat sheet as modelled here, will result in a «hot spot» of lower temperature than these calculations give because the heat flow will spread out on this way to the skin.

Hot veins associated with the tumour but passing close to the skin provide a major means of detection in practice and will presumably be still effective if the vein comes nearer to the skin than the oedematous region.

REFERENCES

1. BARKER J.R.: Heat flow simulations for breasts with cancer. Report: University of Bath, Aug. 1976.

Tab. I. **Factors influencing skin temperature.**

Parameters	Dermis	Fatty tissue	Oedematous fatty tissue
Conductivity W $m^{-1}K^{-1}$	0.42	0.25	0.62
* Perfusion constant kg $m^{-3}s^{-1}$	0.16	0.2	0.04
** Metabolic rate W m-3	840	840	168
Specific heat of blood = 3900 J kg-'K-1			
Heat transfer coefficient, skin to ambient = 13.6 W $m^{-2}K^{-1}$			

* The «perfusion constant» equals the mass of blood perfusing unit vol. of tissue per unit time.
** «Metabolic rate» is the thermal power generated chemically per unit vol.; the values shown are only an order of magnitude figure, namely, 0.0002 cal/(cc. sec) = 840 W m^{-3}.

CASE REPORT

Hematoma of the breast

by W. VAS, D. McLOUGHLIN and J. DAVIDSON

Department of Radiology, Henderson General Hospital, Hamilton, Ontario (Canada)

A) INTRODUCTION

The patient, an obese 71 yrs old white female, developed deep venous thrombosis of the right leg for which she was heparinized and subsequently put into oral anti-coagulant treatment. Two months later she developed a painful, reddish swelling of her right breast which went on to form an ulcerated area, covered with a heavy black eschar (Fig. 1). There was no history of trauma to the breast. Physical examination revealed a grossly swollen erythematous right breast with an area of necrotic skin 10 cm in diameter and granulation tissue around the edge. The surface of the lesion was dry and it was black in colour. No enlarged axillary nodes were palpable. The clinical impression was that the patient had a large ulcerating carcinoma or had developed a breast hematoma as a result of her anti-coagulant therapy. The possibility of bleeding into a pre-existing breast lesion such as an inflammatory carcinoma was also considered.

Mammography of the right breast showed complete loss of the normal soft tissue planes with a large defect anteriorly. There was increase in density of the remainder of the breast. No calcification was seen (Fig. 2). The appearances were interpreted as a large necrotic area anteriorly with possible underlying neoplastic infiltration in the remainder of the breast. Thermography (T.) of the right breast, however, showed a large irregular cold area, including the periareolar region, with increased heat emission above the cool area. (Fig. 3). In view of the striking T. findings, the possibility of a breast neoplasm seemed less likely and a diagnosis of breast hematoma induced by anti-coagulant treatment with necrosis of the overlying breast tissue and skin was considered. A simple mastectomy was performed.

The resected right breast showed a large necrotic ulcer in the middle of the breast, 10x6 cms, with destruction of the nipple and areola. The adjacent skin appeared slightly pigmented and thickened. The breast tissue measured an average of 5 cm in thickness and showed extensive areas of induration. No tumour mass was identified. Histological sections confirmed the presence of skin ulceration with granulation tissue forming the base of the ulcerated area. There was fat necrosis with a florid granulomatous inflammatory reaction and focal hemorrhages. The necrotic fatty lobules were separated by fibrous septa and within the lobules there was a dense infiltrate

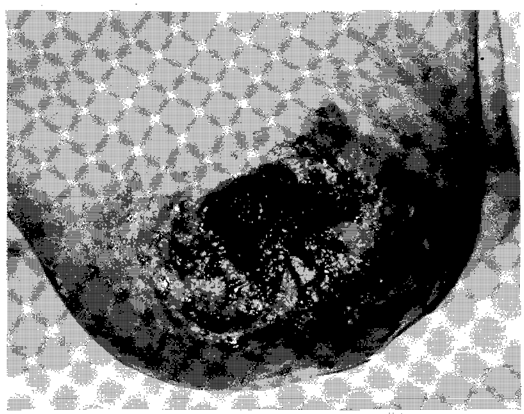

Fig. 1. The right breast is markedly swollen with a large necrotic ulcer in the middle of the breast and destruction of the nipple and areola. The adjacent skin is discoloured and indurated.

of histiocytic cells, many with foamy cytoplasm and large numbers of multinucleate cells of the foreign body type. The residual recognizable breast tissue consisted of a few unremarkable mammary ducts. No evidence of malignancy was found.

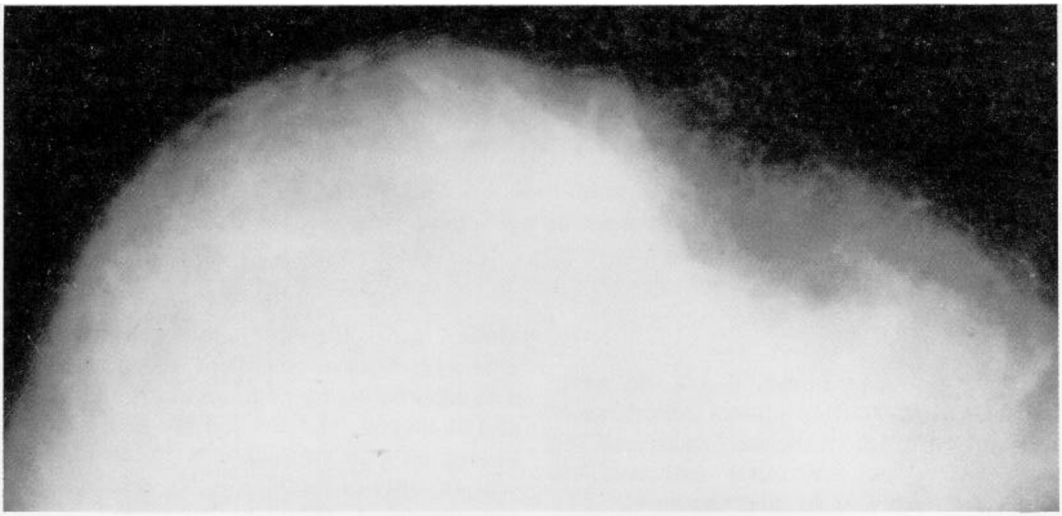

Fig. 2. Mammogram of the right breast shows a large defect anteriorly. There is increase in density in the remainder of the breast.

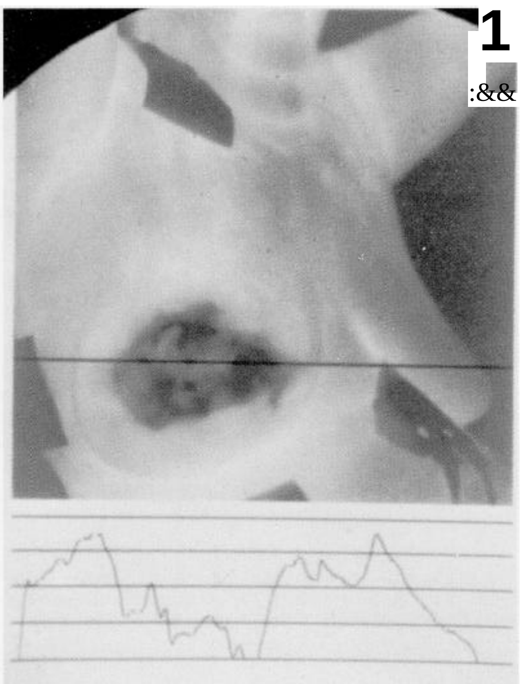

Fig. 3. Thermogram of the right breast shows an illdefined cold area in the area of the breast lesion.

B) DISCUSSION

The development of infarction and necrosis of the skin and subcutaneous tissue is an uncommon complication of anti-coagulant therapy with coumarin derivatives.[1,2] Coumarin necrosis has a marked predilection for areas with abundant subcutaneous fat e.g. buttock, thighs and rarely breast. It occurs between the third and tenth day of therapy and develops almost exclusively in obese females. The lesions appear suddenly and are characterized by pain, erythema, oedema and hemorrhagic bullae, followed by necrosis with development of an overlying black eschar. The underlying breast tissue shows large lobules of fat necrosis with pale yellow discoloration and focal hemorrhages.

T. cannot generally be used to distinguish between benign and malignant lesions because the T. patterns are non-specific. It is not an anatomical detector of cancer but rather an alerter of a physiological disturbance which may be a malignant process which requires corroboration by other methods. Increased heat is often associated with a malignant process. With the newer T. equipment, some therma1 abnormalities can be found in at least 95% of cases of breast neoplasm.[3]

In the case described above, the finding of an irregular cold area in the region of the lesion, in association with the clinical presentation, allowed the radiologist to arrive at the diagnosis of breast hematoma in spite of the mammographic findings.

REFERENCES

1. DICATO M.A., ELLMAN L.: Coumadin (R)-induced necrosis of breast, diseminated intravascular coagulation and hemolytic anemia. *Ann. Intern. Med., 83, 233.234,* 1975.
2. TONG D.: Hemorrhagic necrosis of the breast complicating anticoagulant therapy and mitral stenosis. *Br. J.* Surg., 58, 625-628, 1971.
3. STRAX PH.: Utilization of diagnostic techniques for cancer of the breast early diagnosis. In GHYS R.: *Medical Thermography,* European Press, Bruxelles 1978.

NEW BOOKS

LA RADIOTHERAPIE: by A. Naoum.

It is a booklet on to the general principles of radiotherapy. It is specially devoted to students. It is published by «Presses Universitaires de France» in the series «Que sais je?».

For further information:
Presses Universitaires de France
108, Bd. Saint-Germain
75006 PARIS - FRANCE

«AN OVERVIEW OF LIQUID CRYSTAL AND ELECTRONIC LUMBAR, THORACIC AND CERVICAL THERMOGRAPHY»: by C.E. Wexler.

It is a short monography, also presented as an audiovisual program. An introduction on the basic concepts and on the contact- and infra-red thermographic apparatus is followed by a focusing of the possibilities thermography offers in the evaluation of nervous syndromes of different origin. The booklet is published by Thermographic Services, Inc. Tarzana Ca. (U.S.A.).

For information write to:
Thermographic services inc.;
-19135 Rosita Street;
TARZANA CA. 91856, (U.S. A.)